A modified phase change pseudopotential lattice Boltzmann model

W. Gong[a], Y.Y. Yan[a,b*], S. Chen[a], E. Wright[a]

[a] *Fluids and Thermal Engineering Research Group, Faculty of Engineering, University of Nottingham, Nottingham, UK*

[b] *Center for Fluids and Thermal Engineering, University of Nottingham Ningbo, China*

Corresponding author: yuying.yan@nottingham.ac.uk

Abstract

Amongst all the multiphase models in the lattice Boltzmann (LB) community, the pseudopotential model has been the most popular approach due to its simplicity and high-efficiency. Recently a number of liquid-vapour phase change models were also proposed based on the pseudopotential LB model. Our study finds that most of the published pseudopotential phase change models rely on an entropy-based energy equation, while the entropy-based energy equation is derived with the equation of state of ideal gas. That means this entropy-based energy equation is not completely suitable for multiphase flow which applies non-ideal equation of state for the phase separation simulation. Therefore a new phase change LB model is proposed in this work, where an improved pseudopotential multiphase model (Li et al., 2013) and a modified energy equation which is solved in the classical fourth-order Runge-Kutta scheme are coupled in a hybrid scheme. The results show that the numerical simulation can capture the basic liquid-vapour phase change features. The D^2 law for droplet evaporation is validated and the square of diameter variation is in good agreement with experimental data. Moreover, the three boiling stages (nucleate boiling, transition boiling and film boiling) are accomplished using the modified model, and the corresponding transient heat fluxes are presented.

Keywords:

1. Introduction

In the past few decades, the lattice Boltzmann (LB) method as an unconventional CFD approach based on kinetic theory has been developed dramatically to be a remarkable numerical tool, especially in the area of mesoscale flow and heat transfer simulation [1–4]. Due to its advantages such as explicit scheme, parallel computing and simple boundary treatment, LB has been widely applied in flow and heat transfer phenomena for single/multi- phase fluid, rarefied gas, phase change, etc [5–12]. Amongst all the LB community members in the field of multiphase flow, the pseudopotential LB model which was first proposed by Shan and Chen [13, 14] has shown tremendous superiority because of its simplicity, versatility and the distinctive feature of automatic phase separation without any specific techniques for interface capturing or tracking. Correspondingly, the LB simulations of liquid-vapour phase change based on the pseudopotential model have drawn more and more attention.

The first liquid-vapour phase change LB model based on pseudopotential model might be attributed to Zhang and Chen [15], who presented the model which has the capability of thermodynamic multiphase flow simulation and successfully achieved liquid-vapour boiling process. Then Hazi and Markus [16] proposed another thermal pseudopotenial model in which an energy equation depicting the local balance law for entropy was coupled. They derived the target temperature equation from the entropy based energy equation and the thermodynamic relationship of non-ideal gases, and gave the corresponding thermal LB equation. Evaporation through a plane interface and two-phase Poiseuille flow were simulated using their thermal LB model [17]. Biferale et al. [18] presented an LB based thermal model in multiphase flow (boiling) and performed a series of 3D simulations at the Rayleigh number Ra $\sim 10^7$. The exponential-form pseudopotential was adopted

in their model and the non-ideal equation of state was not employed. Gong and Cheng [19, 20] proposed an LB phase change model for simulation of pool boiling. This model has been used to study bubble nucleation, growth, departure, and surface wettability effects on pool boiling heat transfer [21, 22], and also been applied to simulate film condensation [23]. Study from Li and Luo [24] showed that the error term in the recovered energy equation by thermal LB equation can generate nonnegligible numerical errors, and then Li et al. [25] developed a new thermal pseudopotential LB model in a hybrid scheme where the entropy based temperature equation was solved by a finite-difference method. Recently Li at al. [26] points out the replacement of $\nabla \cdot (\lambda \nabla T) / \rho c_v$ with $\nabla \cdot (\alpha \nabla T)$ in some existing thermal LB models is not appropriate. They then improved the thermal LB model for liquid-vapour phase change and some error terms existing in the recovered macroscopic temperature equation in some models are also eliminated in their model. Our latest work [27] studied the feature of single-component multiphase pseudopotential LB models that a steady multi-bubble/droplet configuration is inaccessible using most of such models, and we thought the most likely reason for that might be the essential attractive interaction forces. After discussion with other researchers, we think that problem still needs further investigation. In addition, the unsteady transition between different bubbles proceeds slowly and has little difference on simulation of boiling process.

In this work, we found that most of the pseudopotential thermal LB models are related to the entropy based energy equation, where the obvious feature is the existence of the term $\frac{T}{\rho c_v}\left(\frac{\partial p_{EOS}}{\partial T}\right)_\rho \nabla \cdot \mathbf{v}$ in the recovered macroscopic energy equation. However, it is found that the derivation of this term is paradoxical, when the equations of state for both ideal gas and non-ideal gas are applied simultaneously. Therefore our work aims at proposing an improved thermal LB model for liquid-vapour phase change by modifying the energy equation in the existing models. Since it has been widely

reported a convection-diffusion equation cannot be completely recovered by a standard thermal LB equation [24, 28–30], a hybrid thermal LB scheme for liquid-vapour phase change is employed to avoid the numerical errors of the thermal LB equation. The present paper is organized as follows. The energy equations used in existing thermal LB models are discussed in Sec. 2. The numerical model and simulation using the modified thermal LB model are presented in Sec. 3, followed by conclusions in Sec 4.

2. The energy equation

The most commonly used recovered energy equation in the thermal LB models mentioned above for liquid-vapour phase change are

$$\partial_t T + \mathbf{v} \cdot \nabla T = \frac{1}{\rho c_v} \nabla \cdot (\lambda \nabla T) - \frac{T}{\rho c_v} \left(\frac{\partial p_{EOS}}{\partial T} \right)_\rho \nabla \cdot \mathbf{v} \tag{1}$$

$$\partial_t T + \mathbf{v} \cdot \nabla T = \nabla \cdot (\alpha \nabla T) - \frac{T}{\rho c_v} \left(\frac{\partial p_{EOS}}{\partial T} \right)_\rho \nabla \cdot \mathbf{v} \tag{2}$$

where $T, \mathbf{v}, \rho, c_v, \lambda, p$ and α are temperature, velocity, density, specific heat at constant volume, thermal conductivity, pressure and thermal diffusivity, respectively. The difference between the two equations is the diffusion term, where in Eq. (2) the volumetric heat ρc_v is treated as a constant in the whole computational field. However, the density changes significantly in the liquid-vapour interface area, which means such simplification theoretically is not an appropriate approach in terms of the physical mechanism. Now attention turns to Eq. (1), which was summarized using the local balance law for entropy by Anderson et al. [31]. The local balance law for entropy can be given as

$$\rho T \frac{ds}{dt} = \nabla \cdot (\lambda \nabla T) \tag{3}$$

where s represents the entropy, and the viscous heat dissipation is neglected. $d/dt = \partial_t + \mathbf{v} \cdot \nabla$ is the material derivative. With the addition of the entropy differential equation using T and v as the independent variables

$$ds = \frac{c_v}{T} dT + \left(\frac{\partial p}{\partial T}\right)_v dv \tag{4}$$

where v is the specific volume, we can derive the entropy based temperature equation Eq. (1).

The derivation of Eq. (1) all seems correct, however, the origin of the entropy local balance law is neglected in this process. The well known macroscopic energy equation in terms of internal energy can be written as (viscous heat dissipation neglected) [15]

$$\rho \left(\partial_t e + \mathbf{v} \cdot \nabla e\right) = -p \nabla \cdot \mathbf{v} + \nabla \cdot \left(\lambda \nabla T\right) \tag{5}$$

where $e = c_v T$ is the internal energy. According to the continuity equation, the compression work term can be transformed

$$p \nabla \cdot \mathbf{v} = -\frac{p}{\rho} \frac{d\rho}{dt} = p\rho \frac{dv}{dt} \tag{6}$$

When combined with the ideal gas equation of state $p = \rho R T$, the thermodynamic relation can be simplified as

$$ds = \frac{c_v}{T} dT + \frac{p}{T} dv \tag{7}$$

From Eq. (5), (6), and (7), the entropy local balance law Eq. (3) can be obtained. It should be noted that the specific heat c_v is treated as a constant.

The derivation process of Eq. (1) from the basic energy transport equation Eq. (5) is given in detail, where we can easily find that the ideal gas equation of state $p = \rho R T$ is indispensable in the whole process. However, in the liquid-vapour phase change pseudopotential LB models, non-ideal

equation of state should be used to realize phase change, which is inconsistent with the ideal gas equation of state. Therefore, following reference [15], the energy transport equation in terms of internal energy neglecting viscous heat dissipation is employed in our model, which can be written as

$$\partial_t T + \mathbf{v} \cdot \nabla T = \frac{1}{\rho c_v} \nabla \cdot (\lambda \nabla T) - \frac{p}{\rho c_v} \nabla \cdot \mathbf{v} \tag{8}$$

3. Numerical Simulation

3.1. Numerical model

Li et al. [32] presented an improved forcing scheme for pseudopotential LB models to eliminate the thermodynamic inconsistency which exists in original pseudopotential LB models by adjusting the mechanical stability condition. In our work, this Li Qing model is adopted for fluid flow simulation.

Many previous works have shown that Multi-Relaxation-Time (MRT) collision operator performs much better than the Bhatnagar-Gross-Krook (BGK) scheme as far as numerical stability is concerned [4, 25, 33, 34]. The following equation shows the LB equation with MRT collision operator

$$f_\alpha \left(\boldsymbol{x} + \boldsymbol{e}_\alpha \delta_t, t + \delta_t \right) = f_\alpha \left(\boldsymbol{x}, t \right) - \left(\mathbf{M^{-1} \Lambda M} \right)_{\alpha\beta} \left(f_\beta - f_\beta^{eq} \right) + \delta_t F'_\alpha \tag{9}$$

where f_α is the density distribution function, the superscript eq means the equilibrium state, $\boldsymbol{x}$ is the spacial location, $\boldsymbol{e}_\alpha$ is the discrete velocity, δ_t is the time step, $\mathbf{M}$ is an orthogonal transformation matrix, $\mathbf{\Lambda} = \left(\tau_\rho^{-1}, \tau_e^{-1}, \tau_\zeta^{-1}, \tau_j^{-1}, \tau_q^{-1}, \tau_j^{-1}, \tau_q^{-1}, \tau_\nu^{-1}, \tau_\nu^{-1} \right)$ is a diagonal matrix containing the relaxation times, and F'_α is the forcing added to the particles. Eq. (9) can also be written in the following form

$$\mathbf{m}^* = \mathbf{m} - \mathbf{\Lambda} \left(\mathbf{m} - \mathbf{m}^{eq} \right) + \delta_t \left(\mathbf{I} - \frac{\mathbf{\Lambda}}{2} \right) \mathbf{S} \tag{10}$$

where $\mathbf{m} = \mathbf{M}\mathbf{f}$, $\mathbf{m}^{eq} = \mathbf{M}\mathbf{f}^{eq}$, $\mathbf{I}$ is the unit tenser, and $\mathbf{S}$ is the forcing term. $\mathbf{m}^{eq}$ can be calculated by

$$\mathbf{m}^{eq} = \rho\left(1, -2 + 3|\mathbf{v}|^2, 1 - 3|\mathbf{v}|^2, v_x, -v_x, v_y, -v_y, v_x^2 - v_y^2, v_x v_y\right)^T \tag{11}$$

The macroscopic density and velocity can be obtained via

$$\rho = \sum_\alpha f_\alpha, \quad \rho\mathbf{v} = \sum_\alpha \boldsymbol{e}_\alpha f_\alpha + \frac{\delta_t}{2}\mathbf{F} \tag{12}$$

where $\mathbf{F}$ is the total force including the buoyancy force $\mathbf{F}_b$ and particle interaction force $\mathbf{F}_m$, which are respectively given by

$$\mathbf{F}_b = (\rho - \rho_{ave})\,\mathbf{g} \tag{13}$$

$$\mathbf{F}_m = -G\psi(\boldsymbol{x})\sum_\alpha w_\alpha \psi(\boldsymbol{x} + \boldsymbol{e}_\alpha)\,\boldsymbol{e}_\alpha \tag{14}$$

where $\mathbf{g}$ is gravity acceleration, ρ_{ave} is the average density in the computational area, G is the particle interaction strength, $\psi(\boldsymbol{x})$ is the pseudopotential, and w_α is the weight. The pseudopotential can be calculated with

$$\psi(\boldsymbol{x}) = \sqrt{\frac{2\left(p_{EOS} - \rho c_s^2\right)}{Gc^2}} \tag{15}$$

where c is the lattice speed, c_s^2 is the lattice sound speed and p_{EOS} is the non-ideal equation of state, for which the Peng-Robinson (P-R) equation of state [35] is adopted

$$p_{EOS} = \frac{\rho RT}{1 - b\rho} - \frac{a\varphi(T)\rho^2}{1 + 2b\rho - b^2\rho^2} \tag{16}$$

where $\varphi(T) = \left[1 + \left(0.37464 + 1.54226\omega - 0.26992\omega^2\right)\left(1 - \sqrt{T/T_c}\right)\right]^2$, $a = 0.45724R^2T_c^2/p_c$, $b = 0.0778RT_c/p_c$ and $\omega = 0.344$. The subscript c denotes critical state. In this work, $a = 3/49$,

$b = 2/21$ and $R = 1$ are utilized, and then $Tc = 0.1094$ can be obtained via calculation. The improved forcing term is given by

$$\mathbf{S} = \begin{bmatrix} 0 \\ 6\mathbf{v}\cdot\mathbf{F} + \dfrac{\sigma|\mathbf{F}_m|^2}{\psi^2\delta_t\left(\tau_e - 0.5\right)} \\ -6\mathbf{v}\cdot\mathbf{F} - \dfrac{\sigma|\mathbf{F}_m|^2}{\psi^2\delta_t\left(\tau_\zeta - 0.5\right)} \\ F_x \\ -F_x \\ F_y \\ -F_y \\ 2\left(v_xF_x - v_yF_y\right) \\ \left(v_xF_y + v_yF_x\right) \end{bmatrix} \tag{17}$$

where $\sigma = 1.2$ is employed in the present work for tuning the mechanical stability condition.

For the temperature equation, Eq. (8) is solved using the classical fourth-order Runge-Kutta scheme [36]. The temperature equation is rewritten as

$$\partial_t T = -\mathbf{v}\cdot\nabla T + \frac{1}{\rho c_v}\nabla\cdot\left(\lambda\nabla T\right) - \frac{p}{\rho c_v}\nabla\cdot\mathbf{v} \tag{18}$$

and the right-hand of this equation is labelled by $K\left(T\right)$. The time discretization is

$$T^{t+\delta t} = T^t + \frac{\delta_t}{6}\left(h_1 + 2h_2 + 2h_3 + h_4\right) \tag{19}$$

where h_1, h_2, h_3, and h_4 are in the following forms, respectively

$$h_1 = K\left(T^t\right),\ h_2 = K\left(T^t + \frac{\delta_t}{2}h_1\right),\ h_3 = K\left(T^t + \frac{\delta_t}{2}h_2\right),\ h_4 = K\left(T^t + \delta_t h_3\right) \tag{20}$$

3.2. Results and discussion

3.2.1. Liquid-vapour coexistent densities

In thermodynamic equilibrium, one basic consistency is that pressure cannot increase with volume, however, this is always violated in analytic models for ideal gases, for example, in the Peng-Robinson equation of state used in our thermal LB model as shown in Fig. 1. Then the Maxwell construction was utilized to correct this deficiency [19]. Fig. 1 gives the Maxwell construction for a steady droplet (diameter 60) with vapour surrounded in a 200×200 computational domain at saturated temperature $Ts = 0.86Tc$. Following the work from Li et al. [25], the kinematic viscosities for liquid and vapour two phases are set as $\nu_L = 0.1$ and $\nu_V = 0.5/3$, the specific heat is taken as a constant $c_v = 6$, and the conductivity is $\lambda = \rho c_v \chi$ with $c_v\chi = 0.028$. All the parameters are given in the lattice unit. With the definition of the relations between lattice units and the physical units, lattice mass $M = 4.1 \times 10^{-10} kg$, lattice length $L = 1.675 \times 10^{-6} m$ and lattice time $T_t = 2.264 \times 10^{-6} s$, the physical values can be obtained as $\rho_L = 950 kg/m^3$, $\nu_L = 1.239 \times 10^{-7} m^2/s$. All the other physical values can also be obtained via simple calculations. In Fig. 1, the curve for ideal equation of state and the straight line for Maxwell construction enclose two regions which have the same area $A1 = A2$, and the two intersections in the left side and in the right side correspond to the coexistent liquid density and vapour density respectively under the same pressure. The asterisks are the coexistent liquid-vapour densities obtained by simulation. The results show that the simulation agrees well with the theoretical analysis for liquid-vapour coexistent densities and the coexistent densities are about $\rho_L \approx 6.50$ and $\rho_V \approx 0.38$, respectively.

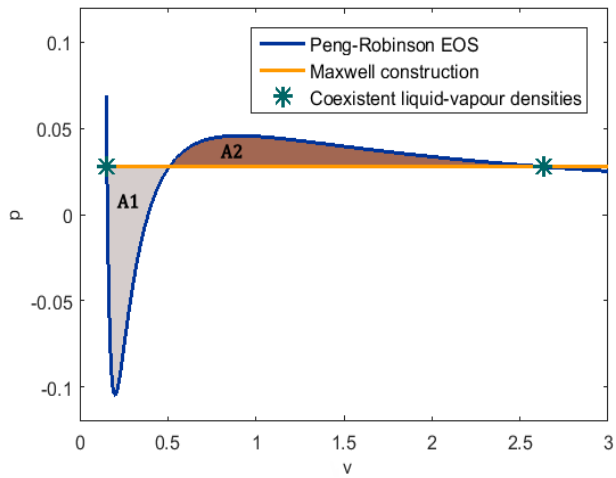

Figure 1: Liquid-vapour coexistent densities and Maxwell construction at $Ts = 0.86Tc$.

3.2.2. D^2 law for droplet evaporation

D^2 law is a well known principle for droplet evaporation and combustion, which describes that the change of droplet diameter over time is linear [37]. The droplet evaporation is implemented in this section for numerical model validation via the D^2 law. The simulation setting is almost the same as those in the previous section, except that the saturated temperature $Ts = 0.86Tc$ is given to the droplet but a higher temperature $Tv = Ts + 0.0137$ is loaded on the vapour region and the boundaries are kept at the temperature Tv. In addition, for D^2 law the thermalphysical parameters should be constant thus thermal conductivity is chosen to be constant with $\lambda = 2/3$.

Fig. 2 gives the transient droplet states with initial diameter $D_0 = 80$ during the evaporation process. It can be clearly seen the diameter of the droplet decreases over time, and the vapour concentration increases around the droplet. The simulated variations of $(D/D_0)^2$ with respect to time for droplets with different initial diameters are shown in Fig. 3(a). It can be concluded from the figure that after a short period of initial time, the square of diameters vary linearly over time, which is consistent with the experimental result from Nishiwaki [38] (see Fig. 3(b)).

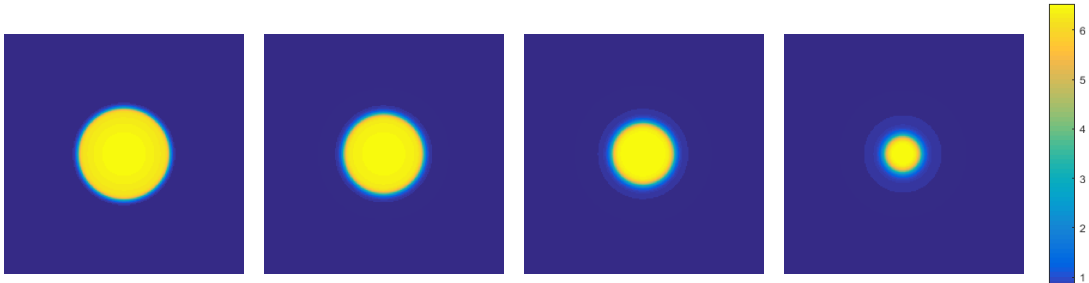

(a) (b) (c) (d)

Figure 2: Snapshots of droplet evaporation, density distribution for $D_0 = 80$ at (a) $t = 10,000$ (b) $t = 60,000$ (c) $t = 110,000$ (d) $t = 160,000$.

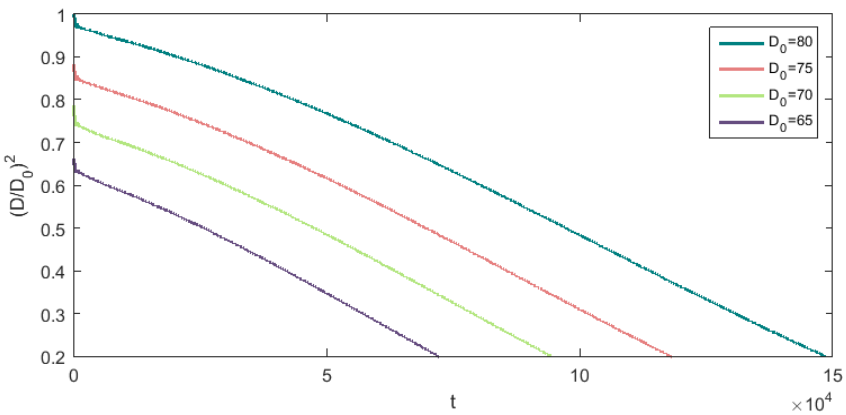

(a)

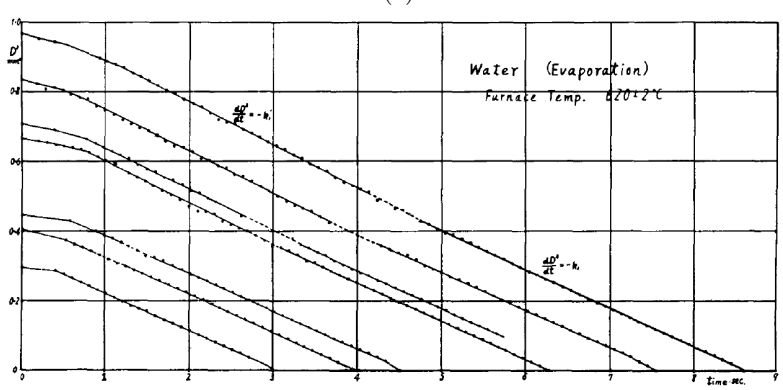

(b)

Figure 3: (a) Simulation of droplets evaporation with different initial diameters (b) Experimental data from Nishiwaki [38], with permission from Elsevier, Copyright 1955.

3.2.3. Three boiling stages

It is well known that there are three distinct boiling stages for pool boiling, i.e. nucleate boiling, transition boiling and film boiling [39]. Study of the three boiling stages is of great significance. Nucleate boiling has been recognized as one of the most effective heat transfer approaches and the critical heat flux for nucleate boiling has long been concerned for heat transfer enhancement. In this work, modelling of the three boiling stages is accomplished using our modified liquid-vapour phase change thermal LB model by controlling the temperature of heating surface. The computational domain is set as 400×180 with upper half domain for vapour and lower half domain for liquid as initial conditions. The top and bottom boundaries are set as non-slip solid, and periodical boundaries are applied in the x direction. The saturated temperature $Ts = 0.86Tc$ is adopted to all the computational domain except that a higher temperature with superheat ΔT is applied to the bottom solid boundary to heat the saturated liquid. The equilibrium contact angle for a droplet on the solid surface is approximately $44.5°$. Differing from the previous settings, the buoyancy force is considered in this part and the gravity acceleration is taken as $g = 3 \times 10^{-5}$.

Fig. 4-6 display the nucleate boiling, transition boiling and film boiling respectively. Fig. 7 shows the corresponding transient heat fluxes for the three boiling stages calculated by $q(t) = \int_0^{L_x} q_w(x)dx/L_x$ where L_x is the length in x direction and $q_w(x) = -\lambda(\partial T/\partial y)|_{y=0}$. All the displayed pictures are after 20,000 time steps once the boiling stages are steady. And for transition boiling and film boiling, the superheat values are enhanced on the basis of a steady nucleate boiling stage. The nucleate boiling is simulated under the superheat $\Delta T = 0.0137$. It can be seen that owing to the heating loaded on the bottom solid surface, some nucleation sites are formed. Following that the vapour bubbles are formed, grow, coalesce with each other, depart from the heating surface, rise and break at the liquid-vapour interface. Whilst during the whole process the nucleation sites

are clearly separated. The transient heat flux in Fig. 7 for this boiling stage is relatively steady and high. However, when the superheat is increased to $\Delta T = 0.02$, the phase change on the heating surface is more complex as many nucleation sites merge into larger vapour films and there are no apparent individual nucleation sites as shown in Fig. 5, and also its transient heat flux becomes unsteady. Finally the superheat $\Delta T = 0.025$ is loaded on the heating surface and when it runs to steady the whole heating solid surface is covered by a large portion of continuous vapour film. The only heat transfer between the heating solid surface and the bulk liquid are conduction and convection in the vapour phase, which leads to a relatively low heat transfer compared to the other two boiling stages as shown in Fig. 7.

4. Conclusions

In this paper we firstly point out that the derivation of the term $\frac{T}{\rho c_v}\left(\frac{\partial p_{EOS}}{\partial T}\right)_\rho \nabla \cdot \mathbf{v}$ existing in the recovered macroscopic energy equation in most of the normally used pseudopotential thermal LB models for liquid-vapour phase change, is paradoxical because the equations of state for both ideal gas and non-ideal gas are adopted simultaneously in the derivation process. Then a modified thermal pseudopotential LB model for liquid-vapour phase change is proposed in this work. The MRT collision operator with an improved forcing scheme from Li et al. and a modified energy transport equation are coupled. The multiphase model is solved in LB scheme while the classical fourth-order Runge-Kutta scheme is employed for the energy equation therefore the modified model is in a hybrid way.

The multiphase model is validated by Maxwell construction for liquid-vapour coexistent densities at the saturated temperature. Then the droplet evaporation process is simulated and the D^2 law is considered. The droplets are in different initial diameters, and the squares of diameter vary linearly

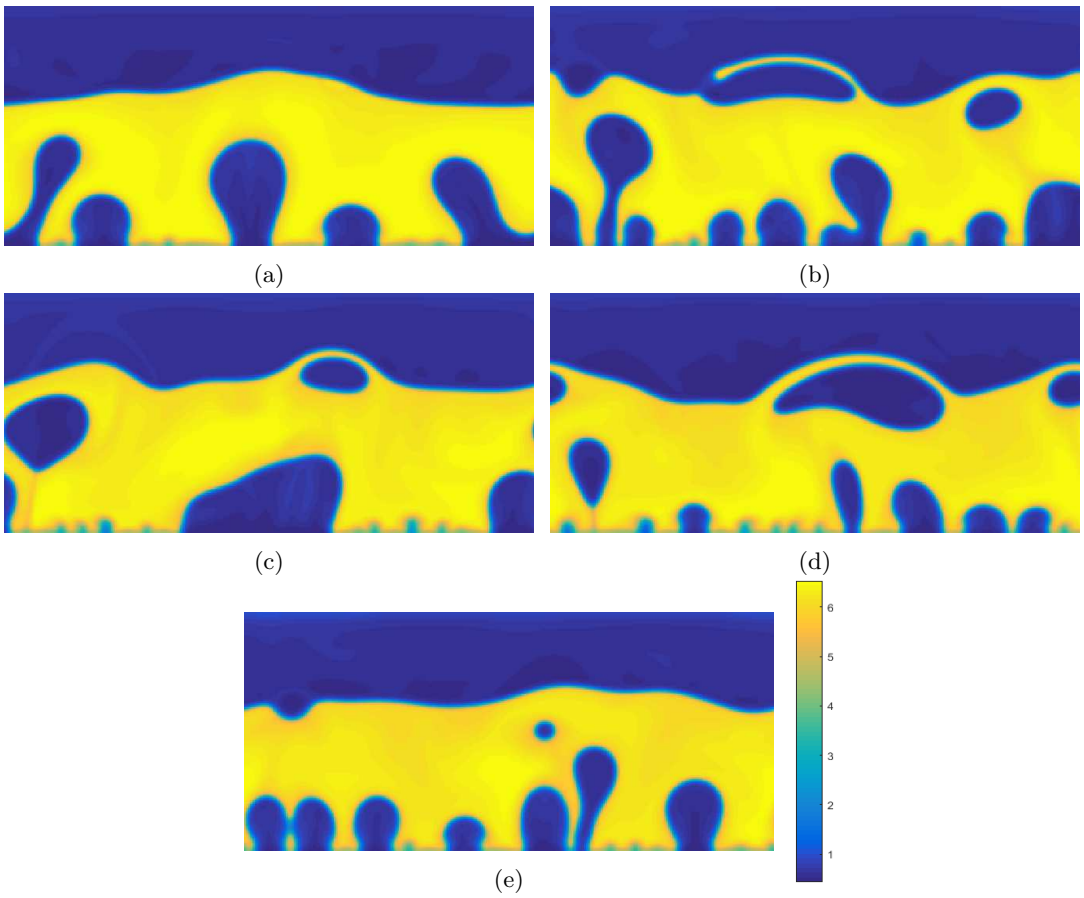

Figure 4: Snapshots of nucleate boiling, density distribution at $\Delta T = 0.0137$ (a) $t = 20,000$ (b) $t = 25,000$ (c) $t = 30,000$ (d) $t = 35,000$ (e) $t = 40,000$.

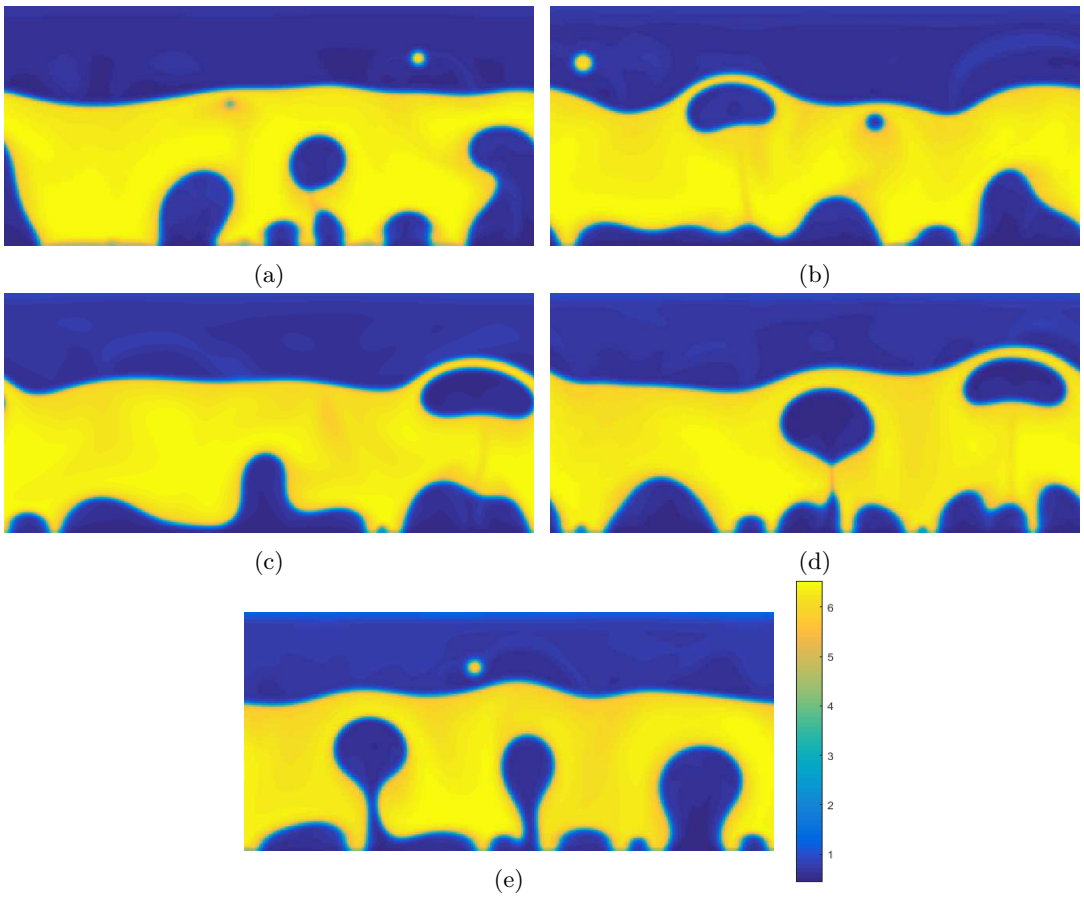

Figure 5: Snapshots of transition boiling, density distribution at $\Delta T = 0.02$ (a) $t = 20,000$ (b) $t = 25,000$ (c) $t = 30,000$ (d) $t = 35,000$ (e) $t = 40,000$.

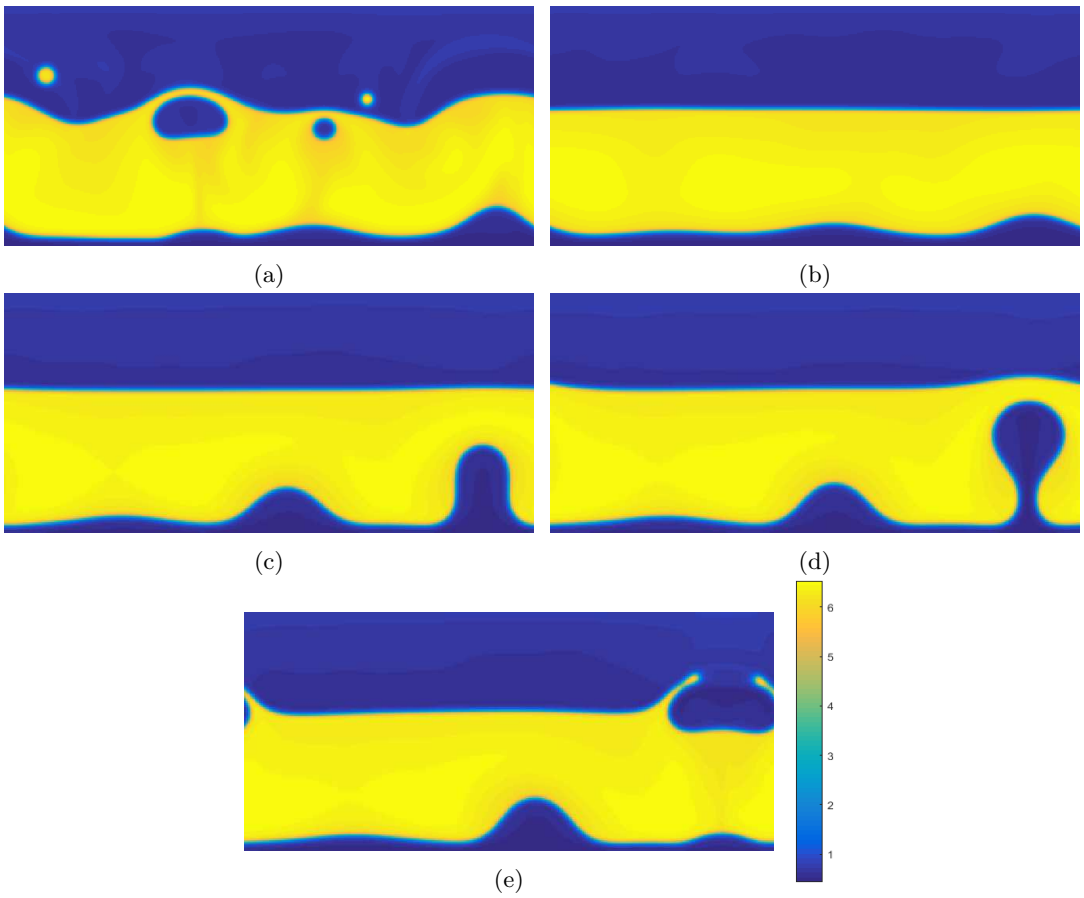

Figure 6: Snapshots of transition boiling, density distribution at $\Delta T = 0.025$ (a) $t = 25,000$ (b) $t = 50,000$ (c) $t = 70,000$ (d) $t = 72,500$ (e) $t = 75,000$.

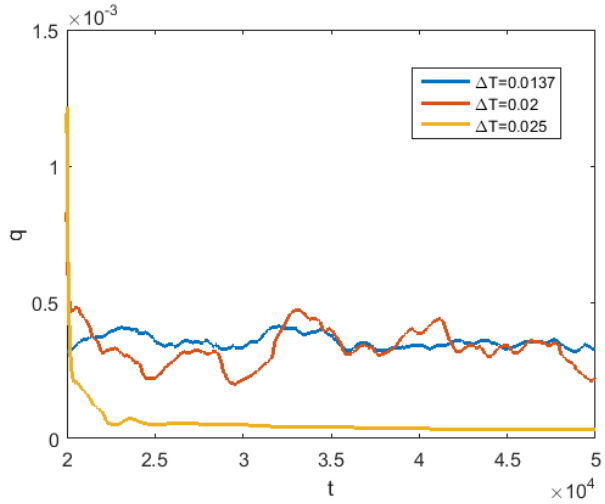

Figure 7: Transient heat fluxes with different superheat conditions.

over time, which is also in good agreement with experimental results from the previously published paper. Finally, the three boiling stages, i.e. nucleate boiling, transition boiling and film boiling are accomplished with different superheat values acting on the bottom solid heating surface using the present model. The transient heat fluxes are given to show the heat transfer features for the three boiling stages. Overall, the modified thermal model, which is based on correct governing equations can be used to capture the basic liquid-vapour phase change features.

Acknowledgements

The authors would like to acknowledge the financial support of this work by the doctoral degree scholarship of China Scholarship Council (CSC) and the University of Nottingham, UK, and this work is also supported by Ningbo Science and Technology Bureau Technology Innovation Team project under Grant No. 2016B10010. The authors would also like to acknowledge the kind help and discussion from Dr Qing Li, Central South university.

References

[1] Shiyi Chen and Gary D Doolen. Lattice boltzmann method for fluid flows. *Annual review of fluid mechanics*, 30(1):329–364, 1998.

[2] MC Sukop. Dt thorne, jr. lattice boltzmann modeling lattice boltzmann modeling. 2006.

[3] Haibo Huang, Michael Sukop, and Xiyun Lu. *Multiphase lattice Boltzmann methods: Theory and application*. John Wiley & Sons, 2015.

[4] T Kruger, H Kusumaatmaja, A Kuzmin, O Shardat, G Silva, and EM Viggen. The lattice boltzmann methods: Principles and practice, 2017.

[5] Linlin Fei and Kai Hong Luo. Consistent forcing scheme in the cascaded lattice boltzmann method. *Physical Review E*, 96(5):053307, 2017.

[6] Haihu Liu, Lei Wu, Yan Ba, and Guang Xi. A lattice boltzmann method for axisymmetric thermocapillary flows. *International Journal of Heat and Mass Transfer*, 104:337–350, 2017.

[7] GH Tang, HH Xia, and Y Shi. Study of wetting and spontaneous motion of droplets on microstructured surfaces with the lattice boltzmann method. *Journal of Applied Physics*, 117(24):244902, 2015.

[8] Li Chen, Qinjun Kang, Yutong Mu, Ya-Ling He, and Wen-Quan Tao. A critical review of the pseudopotential multiphase lattice boltzmann model: Methods and applications. *International Journal of Heat and Mass Transfer*, 76:210–236, 2014.

[9] Wei Gong, Yingqing Zu, Sheng Chen, and Yuying Yan. Wetting transition energy curves for a droplet on a square-post patterned surface. *Science Bulletin*, 62(2):136–142, 2017.

[10] Wei Gong, Yuying Yan, Sheng Chen, and Donald Giddings. Numerical study of wetting transitions on biomimetic surfaces using a lattice boltzmann approach with large density ratio. *Journal of Bionic Engineering*, 14(3):486–496, 2017.

[11] Linlin Fei, Kai Hong Luo, Chuandong Lin, and Qing Li. Modeling incompressible thermal flows using a central-moments-based lattice boltzmann method. *International Journal of Heat and Mass Transfer*, 120:624–634, 2018.

[12] Wei Gong, Sheng Chen, and Yuying Yan. A thermal immiscible multiphase flow simulation by lattice boltzmann method. *International Communications in Heat and Mass Transfer*, 88:136–138, 2017.

[13] Xiaowen Shan and Hudong Chen. Lattice boltzmann model for simulating flows with multiple phases and components. *Physical Review E*, 47(3):1815, 1993.

[14] Xiaowen Shan and Hudong Chen. Simulation of nonideal gases and liquid-gas phase transitions by the lattice boltzmann equation. *Physical Review E*, 49(4):2941, 1994.

[15] Raoyang Zhang and Hudong Chen. Lattice boltzmann method for simulations of liquid-vapor thermal flows. *Physical Review E*, 67(6):066711, 2003.

[16] Gabor Hazi and Attila Markus. On the bubble departure diameter and release frequency based on numerical simulation results. *International Journal of Heat and Mass Transfer*, 52(5):1472–1480, 2009.

[17] Attila Márkus and Gábor Házi. Simulation of evaporation by an extension of the pseudopotential lattice boltzmann method: A quantitative analysis. *Physical Review E*, 83(4):046705, 2011.

[18] L Biferale, P Perlekar, M Sbragaglia, and F Toschi. Convection in multiphase fluid flows using lattice boltzmann methods. *Physical Review Letters*, 108(10):104502, 2012.

[19] Shuai Gong and Ping Cheng. A lattice boltzmann method for simulation of liquid–vapor phase-change heat transfer. *International Journal of Heat and Mass Transfer*, 55(17):4923–4927, 2012.

[20] Shuai Gong and Ping Cheng. Lattice boltzmann simulation of periodic bubble nucleation, growth and departure from a heated surface in pool boiling. *International Journal of Heat and Mass Transfer*, 64:122–132, 2013.

[21] Shuai Gong, Ping Cheng, and Xiaojun Quan. Two-dimensional mesoscale simulations of saturated pool boiling from rough surfaces. part i: Bubble nucleation in a single cavity at low superheats. *International Journal of Heat and Mass Transfer*, 100:927–937, 2016.

[22] Shuai Gong and Ping Cheng. Two-dimensional mesoscale simulations of saturated pool boiling from rough surfaces. part ii: Bubble interactions above multi-cavities. *International Journal of Heat and Mass Transfer*, 100:938–948, 2016.

[23] Xiuliang Liu and Ping Cheng. Lattice boltzmann simulation of steady laminar film condensation on a vertical hydrophilic subcooled flat plate. *International Journal of Heat and Mass Transfer*, 62:507–514, 2013.

[24] Qing Li and KH Luo. Effect of the forcing term in the pseudopotential lattice boltzmann modeling of thermal flows. *Physical Review E*, 89(5):053022, 2014.

[25] Qing Li, QJ Kang, Marianne M Francois, YL He, and KH Luo. Lattice boltzmann modeling of boiling heat transfer: The boiling curve and the effects of wettability. *International Journal of Heat and Mass Transfer*, 85:787–796, 2015.

[26] Qing Li, P Zhou, and HJ Yan. Improved thermal lattice boltzmann model for simulation of liquid-vapor phase change. *arXiv preprint arXiv:1709.04400*, 2017.

[27] Wei Gong, Yuying Yan, and Sheng Chen. A study on the unphysical mass transfer of scmp pseudopotential lbm. *International Journal of Heat and Mass Transfer*, 123:815–820, 2018.

[28] B Chopard, JL Falcone, and J Latt. The lattice boltzmann advection-diffusion model revisited. *The European Physical Journal-Special Topics*, 171(1):245–249, 2009.

[29] Zhenhua Chai and TS Zhao. Lattice boltzmann model for the convection-diffusion equation. *Physical Review E*, 87(6):063309, 2013.

[30] Rongzong Huang and Huiying Wu. A modified multiple-relaxation-time lattice boltzmann model for convection–diffusion equation. *Journal of Computational Physics*, 274:50–63, 2014.

[31] Daniel M Anderson, Geoffrey B McFadden, and Adam A Wheeler. Diffuse-interface methods in fluid mechanics. *Annual review of fluid mechanics*, 30(1):139–165, 1998.

[32] Q Li, KH Luo, XJ Li, et al. Forcing scheme in pseudopotential lattice boltzmann model for multiphase flows. *Physical Review E*, 86(1):016709, 2012.

[33] Pierre Lallemand and Li-Shi Luo. Theory of the lattice boltzmann method: Dispersion, dissipation, isotropy, galilean invariance, and stability. *Physical Review E*, 61(6):6546, 2000.

[34] YH Qian, Dominique d'Humières, and Pierre Lallemand. Lattice bgk models for navier-stokes equation. *EPL (Europhysics Letters)*, 17(6):479, 1992.

[35] Peng Yuan and Laura Schaefer. Equations of state in a lattice boltzmann model. *Physics of Fluids*, 18(4):042101, 2006.

[36] Kendall E Atkinson. *An introduction to numerical analysis.* John Wiley & Sons, 2008.

[37] CK Law. Recent advances in droplet vaporization and combustion. *Progress in energy and combustion science*, 8(3):171–201, 1982.

[38] Niichi Nishiwaki. Kinetics of liquid combustion processes: evaporation and ignition lag of fuel droplets. In *Symposium (International) on Combustion*, volume 5, pages 148–158. Elsevier, 1955.

[39] Long Sun Tong and Yu S Tang. *Boiling heat transfer and two-phase flow.* CRC press, 1997.